

2009

Tunable Photonic Microwave Filters Based on Opto-VLSI Processors

Feng Xiao

Edith Cowan University

Budi Juswardy

Edith Cowan University

Kamal Alameh

Edith Cowan University

10.1109/LPT.2009.2016979

This article was originally published as: Xiao, F., Juswardy, B., & Alameh, K. (2009). Tunable Photonic Microwave Filters Based on Opto-VLSI Processors. *IEEE Photonics Technology Letters*, 21(11), 751-753. Original article available [here](#)

© 2009 IEEE. Personal use of this material is permitted. Permission from IEEE must be obtained for all other uses, in any current or future media, including reprinting/republishing this material for advertising or promotional purposes, creating new collective works, for resale or redistribution to servers or lists, or reuse of any copyrighted component of this work in other works.

This Journal Article is posted at Research Online.

<http://ro.ecu.edu.au/ecuworks/567>

Tunable Photonic Microwave Filters Based on Opto-VLSI Processors

Feng Xiao, Budi Juswardy, and Kamal Alameh

Abstract—A tunable photonic microwave filter structure utilizing an opto-very-large scale integration (opto-VLSI) processor is proposed and experimentally demonstrated. The opto-VLSI processor slices a radio-frequency (RF)-modulated wideband light source into wavebands of arbitrary weights and incremental delay times to realize a tunable RF filter response. Experimental results demonstrate a tunable microwave filter that can simply be reconfigured with high flexibility via a software-driven opto-VLSI processor. Theoretical simulations are in good agreement with the experimental results.

Index Terms—Microwave photonics, optical processing of microwave signals, photonic microwave filters, spatial light modulator.

I. INTRODUCTION

PHOTONICS-BASED processing of microwave and millimeter-wave signals is a powerful technique that offers advantages such as ultrawide bandwidth, immunity to electromagnetic interference, flexibility, and lightweight [1]–[3].

In recent years, numerous reconfigurable coherent-free photonic microwave transversal filter structures have been proposed and demonstrated, where a multiwavelength source is employed to suppress the optical interference in conjunction with modifying the optical tap weights or the time-delay increment between taps [4]–[10]. Spectral slicing of a radio-frequency (RF)-modulated broadband optical source has been employed to generate different wavebands. However, the use of Bragg gratings or arrayed waveguide gratings for realizing spectral slicing results in fixed time-delay increments, which limit the tunability of the photonic microwave transversal filter. Another approach to generating optical taps is the use of a tunable laser array, where each tunable laser element is dedicated to control the weight of a single optical tap. However, the main disadvantage of this approach is the high cost and reliability of the filter structure, especially when the number of taps increases.

As a powerful spatial-light modulation technology, opto-very-large scale integration (opto-VLSI) has been widely used for photonic RF signal processing [11]–[13]. This technology can provide high-precision weight control for a large number of filter taps. However, these all reported opto-VLSI-based transversal filter structures have limited tunability and flexibility because they use fixed (rather than

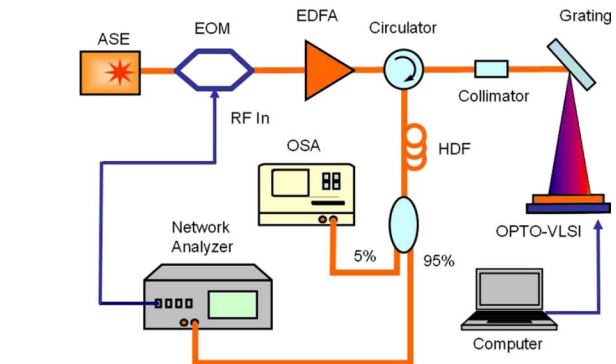


Fig. 1. Experimental setup for the tunable photonic microwave filter structure.

variable) tap separation and tap number. More recently, an opto-VLSI-based tunable optical filter structure has been reported, which demonstrated the ability of opto-VLSI processors to simultaneously control the waveband separation and amplitude [14].

In this letter, we propose and experimentally demonstrate the principle of a novel tunable photonic microwave filter based on the use of an opto-VLSI processor [15]. Through computer-generated phase holograms uploaded onto the opto-VLSI processor, arbitrary spectral slicing with adaptive wavelength separations as well as independent tap weight control can be achieved. This demonstration has a significant advantage that the time-delay increment, tap numbers, and tap weights can be adjusted independently and simultaneously, simply by electronics. To the best of our knowledge, this structure has the highest flexibility compared to previously reported microwave filter structures [13], [14]. The proposed tunable filter structure is a practical solution to realizing flexible and tunable microwave filters.

II. PROPOSED TUNABLE PHOTONIC MICROWAVE FILTERS

In Fig. 1, the proposed tunable photonic microwave filter is illustrated through an experimental setup. A broadband light source of amplified spontaneous emission (ASE) is externally modulated by an RF signal through an electrooptic modulator (EOM). The modulated light is amplified by an erbium-doped fiber amplifier (EDFA) and routed via a circulator into a collimator which collimates the light into a 1-mm diameter beam. A 1200-line/mm grating plate disperses the incident beam into spectral components along different directions and linearly maps them onto the active window of an opto-VLSI processor.

The opto-VLSI processor consists of an array of liquid crystal cells independently addressed by a VLSI circuit to generate multiphase holographic diffraction gratings capable of steering and/or multicasting an optical beam [15]. It is software configured, polarization-independent, cost effective, and very reliable

Manuscript received January 30, 2009; revised February 24, 2009. First published March 16, 2009; current version published May 15, 2009.

The authors are with the Centre for MicroPhotonic Systems, Edith Cowan University, Joondalup, WA, 6027, Australia (e-mail: f.xiao@ecu.edu.au; bjusward@student.ecu.edu.au; k.alameh@ecu.edu.au).

Color versions of one or more of the figures in this letter are available online at <http://ieeexplore.ieee.org>.

Digital Object Identifier 10.1109/LPT.2009.2016979

since beam steering/multicasting is achieved with no mechanically moving part. It also features low power consumption and switching voltage, and a switching speed of 10 ms.

The wavelength of the optical field incident onto the opto-VLSI processor varies along the pixels, which can be logically partitioned into pixel blocks by programming the opto-VLSI processor. The spectral component, falling within the specific pixel block of the opto-VLSI processor, can be either steered back along the incidence path thus coupling it back into the fiber collimator with minimum attenuation, or deliberately steered “off-track” so that its power is partially coupled back into the fiber collimator leading to an appropriate optical attenuation for that spectral component. Therefore, by manipulating the phase hologram of an individual pixel block, the power of each waveband component can be independently adjusted according to the required tap weights; and by partitioning the pixels into appropriate blocks, the optical taps with specific wavelength spacing can be picked out from the wideband light source while all the other wavebands are steered off-track and attenuated dramatically. In other words, by configuring the phase hologram employed to the opto-VLSI processor, tap weights and tap separations can be adjusted simultaneously, independently, and continuously.

The optical taps that are coupled back into the fiber collimator are fed, through the circulator, to a high dispersion optical fiber, where the different RF-modulated wavebands experience different delay times. The delayed RF-modulated wavebands are finally photodetected by a photoreceiver built into a network analyzer, which displays the microwave filter response. An optical spectrum analyzer (OSA) is also used as a monitor driven by a small fraction of the light detected by the photodiode of the network analyzer.

In the experiments, the RF signal generated by the network analyzer was used to intensity modulate the broadband ASE source using a JDS Uniphase EOM of 4-GHz bandwidth. A 256-phase-level 1-D opto-VLSI processor was used, which has 1×4096 pixels, with $1 \mu\text{m}$ pixel size and $0.8 \mu\text{m}$ dead spacing between adjacent pixels. A Labview software was specifically developed to appropriately partition the pixel blocks so that the optimum wavebands are selected. The pixel blocks are then driven by optimized phase holograms (blazed gratings) that steer the selected wavebands so that they are coupled back into the collimator. By optimizing the size and the phase profile of each pixel block, any desirable weight and time-delay increment is synthesized after the wavebands are launched into the high dispersion fiber (HDF), which has dispersion coefficient 382.5 ps/nm and insertion loss 4.6 dB .

The response of the filter structure shown in Fig. 1 can be expressed as [1]

$$H(f) = \sum_{r=0}^M a_r \exp[-j2\pi r f \tau] \quad (1)$$

where f is the RF frequency, M is the number of the detected RF-modulated wavebands, a_r is the r th tap weight, which is proportional to the optical power of the r th waveband, and τ is the time delay between adjacent wavebands introduced by the HDF. The time delay τ can also be expressed in terms of the dispersion of the HDF as

$$\tau = \alpha \cdot \Delta\lambda \quad (2)$$

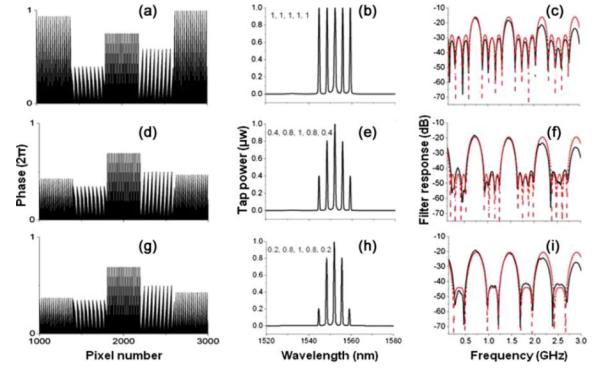


Fig. 2. Microwave filter tuning through tap weight control. (a), (d), and (g) phase hologram applied to the opto-VLSI processor; (b), (e), and (h) selected RF-modulated wavebands; (c), (f), and (i) measured (solid line) and simulated (dashed line) filter responses for each case.

where α denotes the dispersion coefficient of the HDF, and $\Delta\lambda$ is the adjacent waveband separation.

III. EXPERIMENTAL RESULTS AND DISCUSSION

To demonstrate the principle of the photonic microwave filter, five taps were used. Fig. 2(a), (d), and (g) shows the phase holograms applied to the opto-VLSI processor to generate a constant time-delay increment with variable filter weights. The opto-VLSI processor was partitioned into five pixel blocks corresponding to five wavebands, and the size of each pixel block was 400 pixels, resulting in a center-to-center waveband separation of 3.60 nm . For each pixel block, an optimum phase hologram was appropriately uploaded, so that the power level of the specific waveband was attenuated to an appropriate intensity. As shown in Fig. 2(a), an appropriate phase hologram for each pixel block was employed to generate a normalized weight profile of $[1, 1, 1, 1, 1]$. Fig. 2(b) shows the selected wavebands measured by the OSA, and Fig. 2(c) shows the corresponding filter response. Note that the waveband coupled back into the collimator depends on the steering angle associated to this waveband and the numerical aperture of the collimator, and that the separation between adjacent wavebands depends on their pixel block sizes. The measured linewidth for each waveband was about 0.5 nm . Note that the spectral range illuminating each pixel block was around 3.6 nm . However, because this spectral range was diverging, only 0.5 nm of this range was actually steered back and coupled into the collimator. By reconfiguring the phase holograms uploaded onto the various pixel blocks, the filter weights were varied to $[0.4, 0.8, 1, 0.8, 0.4]$, and then to $[0.2, 0.8, 1, 0.8, 0.2]$ as shown in Fig. 2(e) and (h). The corresponding filter responses are shown in Fig. 2(f) and (i), respectively, where changes in rejection band and bandwidth are demonstrated, as a result of waveband attenuation.

Note that in Fig. 2(c), (f), and (i) the solid lines denote the experimental results, which agree well with the simulation results calculated from (1) and (2), shown in dashed lines. All the filter responses shown in Fig. 2 exhibit a free-spectral range (FSR) of about 722 MHz and this is in good agreement with the specified dispersion coefficient of the HDF used in the experiments. The time delay increment, which is the product of the waveband separation and dispersion coefficient of the HDF, was 1.38 ns .

The unique capability of the proposed tunable filter structure is its ability to continuously tune the time delay increment.

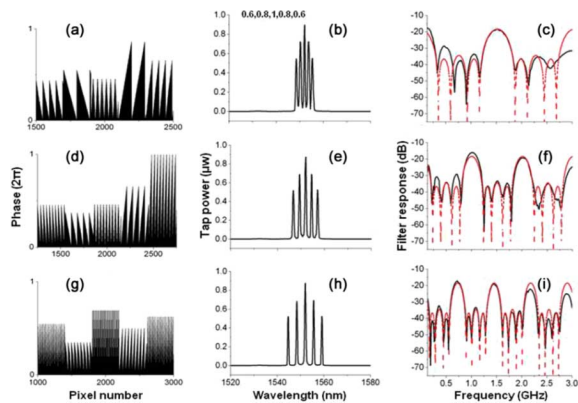


Fig. 3. Microwave filter tuning through time-delay increment control. (a), (d), and (g) phase hologram applied to the opto-VLSI processor; (b), (e), and (h) selected RF-modulated wavebands; (c), (f), and (i) measured (solid line) and simulated (dashed line) filter responses for each case.

This is accomplished by changing the spacing between adjacent pixel blocks (i.e., the pixel block size and center). Fig. 3(a), (d), and (g) shows the phase holograms applied to the opto-VLSI processor to synthesize a normalized weight profile of [0.6, 0.8, 1.0, 0.8, 0.6] but different time delay increments. The corresponding wavebands are shown in Fig. 3(b), (e), and (h). For these three cases, the sizes of the pixel blocks were 200, 300, and 400 pixels, respectively, corresponding to waveband separations of 1.72, 2.60, and 3.60 nm, respectively. Note that by optimizing the phase hologram for each pixel block, a normalized weight profile [0.6, 0.8, 1, 0.8, 0.6] was maintained in all cases. Fig. 3(c), (f), and (i) shows the corresponding measured (solid) and simulated (dashed) filter responses. It is evident from Fig. 3 that the tuning of the waveband separation (i.e., the time delay increment) controls the FSR as well as the bandwidth of the filter. For example, in Fig. 3, the FSR was reduced from 1.52 to 1.01 GHz, and then to 722 MHz, and the filter bandwidth dropped from 216 to 142 MHz and then to 86 MHz, when the time-delay increment was increased from 0.66 to 0.99 ns, and then to 1.38 ns, respectively. Note that a good agreement between the simulated and measured filter responses is displayed in Fig. 3.

By investigating the filter responses shown in Fig. 2(c), (f), (i) and Fig. 3(c), (f), (i), one can see that the spectral response fades remarkably as the RF frequency increases. This is due to the interaction between the dispersion of the HDF and the nonzero optical bandwidth of each waveband [16], [17]. This limitation is inherent to all filters that use spectral slicing. The bandwidth of the sliced wavebands in Figs. 2 and 3 was about 0.5 nm. Preliminary experimental results have shown that a narrower waveband bandwidth can be achieved using a higher dispersion grating plate and/or a larger distance between the grating and the opto-VLSI processor.

Even though the optical tap generation involves fiber to free-space and free-space to fiber coupling, standard passive micro-assembly can be used to realize low-cost, robust, and stable alignment without the need of automated high-precision stages [18]. Note that the maximum number of optical taps that can be generated depends on the bandwidth of the ASE source, the size of the active window of the opto-VLSI processor, and the waveband separation. For our current experimental system, which is

based on the 1-D opto-VLSI processor, up to 12 optical taps with the waveband separation of 2.60 nm can be generated. Note that, by using a 2-D opto-VLSI processor, one can increase the number of optical taps significantly.

IV. CONCLUSION

We have proposed and demonstrated the principle of a novel tunable photonic microwave filter having variable rejection band, bandwidth, and FSR. In particular, a five-tap tunable photonic microwave filter with precisely controllable tap spacing and amplitudes has experimentally been demonstrated through the use of computer-generated phase holograms uploaded onto an opto-VLSI processor.

REFERENCES

- [1] A. J. Seeds and K. J. Williams, "Microwave photonics," *J. Lightw. Technol.*, vol. 24, no. 12, pp. 4628–4641, Dec. 2006.
- [2] J. Capmany, B. Ortega, and D. Pastor, "A tutorial on microwave photonic filters," *J. Lightw. Technol.*, vol. 24, no. 1, pp. 201–229, Jan. 2006.
- [3] R. A. Minasian, "Photonic signal processing of microwave signals," *IEEE Trans. Microw. Theory Tech.*, vol. 54, no. 2, pt. 2, pp. 832–846, Feb. 2006.
- [4] J. Capmany, D. Pastor, and B. Ortega, "New and flexible fiber-optic delay-line filters using chirped Bragg gratings and laser arrays," *IEEE Trans. Microw. Theory Tech.*, vol. 47, no. 7, pt. 2, pp. 1321–1326, Jul. 1999.
- [5] V. Polo, B. Vidal, J. L. Corral, and J. Marti, "Novel tunable photonic microwave filter based on laser arrays and $N \times N$ AWG-based delay lines," *IEEE Photon. Technol. Lett.*, vol. 15, no. 4, pp. 584–586, Apr. 2003.
- [6] A. Ortigosa-Blanch, J. Mora, J. Capmany, B. Ortega, and D. Pastor, "Tunable radio-frequency photonic filter based on an actively mode-locked fiber laser," *Opt. Lett.*, vol. 31, pp. 709–711, 2006.
- [7] D. B. Hunter and L. V. T. Nguyen, "Widely tunable RF photonic filter using WDM and a multichannel chirped fiber grating," *IEEE Trans. Microw. Theory Tech.*, vol. 54, no. 2, pt. 2, pp. 900–905, Feb. 2006.
- [8] G. Ning, P. Shum, and J. Q. Zhou, "Chromatic dispersion effect on microwave photonic filter with a tunable linearly chirped fiber Bragg grating," *Microw. Opt. Tech. Lett.*, vol. 49, pp. 2131–2133, 2007.
- [9] S. R. Blals and J. P. Yao, "Tunable photonic microwave filter using a superstructured FBG with two reflection bands having complementary chirps," *IEEE Photon. Technol. Lett.*, vol. 20, no. 3, pp. 199–201, Feb. 1, 2008.
- [10] J. H. Lee, Y. M. Chang, Y. Han, S. B. Lee, and H. Y. Chung, "Fully reconfigurable photonic microwave transversal filter based on digital micromirror device and continuous-wave, incoherent supercontinuum source," *Appl. Opt.*, vol. 46, pp. 5158–5167, 2007.
- [11] T. Mengual, B. Vidal, and J. Marti, "Continuously tunable photonic microwave filter based on a spatial light modulator," *Opt. Commun.*, vol. 281, pp. 2746–2749, 2008.
- [12] J. Capmany, J. Mora, D. Pastor, and B. Ortega, "High-quality online-reconfigurable microwave photonic transversal filter with positive and negative coefficients," *IEEE Photon. Technol. Lett.*, vol. 17, no. 12, pp. 2730–2732, Dec. 2005.
- [13] R. Zheng, K. Alameh, and Z. Wang, "A tunable photonic RF notch filter based on opto-VLSI technology," *Microw. Opt. Tech. Lett.*, vol. 48, pp. 1011–1015, 2006.
- [14] M. Aljada and K. Alameh, "Reconfigurable multi-passband optical filter using opto-VLSI processor," in *2008 Opto-Electronics and Communications Conf. (OECC)*, 2008, pp. 1–2.
- [15] F. Xiao, B. Juswardy, K. Alameh, and Y. Lee, "Novel broadband reconfigurable optical add-drop multiplexer employing custom fiber arrays and opto-VLSI processors," *Opt. Express*, vol. 16, p. 6, 2008.
- [16] J. D. Taylor, L. R. Chen, and X. J. Gu, "Simple reconfigurable photonic microwave filter using an arrayed waveguide grating and fiber Bragg gratings," *IEEE Photon. Technol. Lett.*, vol. 19, no. 7, pp. 510–512, Apr. 1, 2007.
- [17] D. Pastor, B. Ortega, J. Capmany, S. Sales, A. Martinez, and P. Muñoz, "Optical microwave filter based on spectral slicing by use of arrayed waveguide gratings," *Opt. Lett.*, vol. 28, pp. 1802–1804, 2003.
- [18] G. Baxter *et al.*, "Highly programmable wavelength selective switch based on liquid crystal on silicon switching elements," presented at the Proc. OFC/NFOEC 2006, Anaheim, CA, Paper OTuF2.